

THE STRUCTURE OF MAGNETIC FIELDS IN DARK CLOUDS: INFRARED POLARIMETRY IN B216–217

ALYSSA A. GOODMAN^{1,2}

Astronomy Department, University of California, Berkeley, CA 94720

TERRY J. JONES¹

School of Physics and Astronomy, University of Minnesota, 116 Church Street, S.E., Minneapolis, MN 55455

ELIZABETH A. LADA² AND PHILIP C. MYERS²

Harvard-Smithsonian Center for Astrophysics, 60 Garden Street, Cambridge, MA 02138

Received 1992 March 18; accepted 1992 April 27

ABSTRACT

We present a near-infrared polarization map of background starlight seen through the B216–217 dark cloud in Taurus. The mean direction and dispersion in direction of the polarization vectors observed in the near-infrared are indistinguishable from the direction and dispersion of optical polarization vectors around the periphery of the dark cloud. Measurements of J - and K -magnitudes of the stars observed in the near-infrared imply a range of extinctions $1 \lesssim A_V \lesssim 10$ mag, while the mean A_V for the stars whose polarization has been measured optically is $\lesssim 1$ mag. Assuming that grains in the high- and low-density regions are similar, and are similarly aligned by magnetic fields, then unless the field becomes significantly more nonuniform in denser regions, *our results imply that the dark cloud has no effect on the projected direction of the magnetic field.* If the field does become more nonuniform in the denser portions of the cloud, then the dark cloud is associated with a change in the total energy of the field, but not with any change in the mean direction of the field. Yet, we also find that the degree of polarization in B216–217 and other dark clouds increases more slowly with extinction than expected: if this reduction in polarization efficiency is caused by a drop in alignment and/or polarizing efficiency in denser regions, *it is possible that near-infrared polarization may be relatively insensitive to the field direction in the dense interior of dark clouds.*

Subject headings: dust, extinction — ISM: clouds — ISM: magnetic fields — polarization

1. INTRODUCTION

Magnetic fields can align dust grains in the interstellar medium. Given that dust grains are not perfectly spherical, light passing through a sea of magnetically aligned grains will become partially linearly polarized (Davis & Greenstein 1951; Purcell 1979; see Hildebrand 1988 for a review). Thus, maps of the polarization of background starlight can reveal the structure of the plane-of-the-sky component of magnetic fields in the space between the observer and the background star. In the direction of well-defined extended dark clouds ($A_V > 1$ mag) in our own Galaxy, the distribution of dust along the line of sight peaks at the cloud's distance. So, polarization maps of dark clouds can reveal structure of the magnetic field associated with the clouds.

Over the past several years, many researchers have used optical polarimetry to map out the fields associated with dark clouds, by observing background stars located around the projected cloud periphery, where $A_V \lesssim 1$ mag (see Myers & Goodman 1991 for a summary). The optical polarization maps point to two key properties of the field structure. First, the field component traced by optical polarimetry appears very coherent, in that it does not appear to tangle, or decorrelate, over even an entire dark cloud complex, such as Taurus (see Moneti

et al. 1984; Goodman et al. 1990). And, second, it appears that density enhancements such as dark clouds have no special effect on the observed field direction (Goodman et al. 1990). In the case of highly elongated dark clouds, comparisons of the position angle of the field with the position angle of the cloud show that no particular orientation (e.g., parallel or perpendicular) is favored (e.g., Heyer et al. 1987; Heyer 1988).

Optical polarimetry cannot reveal the field direction within the projected boundary of a “dark” cloud: by definition no background stars are visible. In the near-infrared, where background starlight is polarized by the same dichroism responsible for optical polarization, background stars can be observed through far more extinction. In this paper, we present a near-infrared polarization map of background starlight seen through the B216–217 dark cloud in Taurus. Our aim is to investigate the structure of the field *within* a dark cloud, and to compare it with the larger scale field structure based on optical polarimetry (Heyer et al. 1987; Moneti et al. 1984).

2. DATA

We surveyed the region of interest for suitable background stars using the National Optical Astronomy Observatory (NOAO) near-infrared array camera (IRIM) at Kitt Peak National Observatory (KPNO), and then we measured polarization one star at a time using primarily the Minnesota Infrared Polarimeter (MIRP) on the Infrared Telescope Facility (IRTF).³

¹ Visiting Astronomer at the Infrared Telescope Facility, which is operated by the University of Hawaii under contract to the National Aeronautics and Space Administration.

² Visiting Astronomer at the Kitt Peak National Observatory, operated by the Association of Universities for Research in Astronomy, Inc., under contract with the National Science Foundation.

³ We used MIRP for 17 of the measurements reported in Table 1, and the IRTF's RC 2 polarimetry system for the remaining five.

2.1. Near-Infrared Imaging to Find Background Sources

In January of 1991, using the IRIM camera (cf. Fowler et al. 1987) on the 1.3 m telescope at Kitt Peak, we surveyed the most highly extinguished portions of B216–217 by creating 11 abutting mosaicked images, each with a field of view of about 8' × 8'. Each mosaic represents 64 10-second-long pointings of the camera, which itself contains a 58 × 62 element InSb array. The observing procedure at Kitt Peak was very similar to that described in Lada et al. (1991). All fields were observed using the *K* (2.2 μm) filter, and some were also observed using *J* (1.3 μm) and *H* (1.6 μm) filters. A total of approximately 190 sources were identified in the *K*-band mosaics, and the survey is complete to about 13th magnitude at *K*.

2.2. Near-Infrared Polarimetry with MIRP

Background stars were selected from the sources identified in the KPNO survey of B216–217 using primarily the criteria that the star be (1) brighter than 11th magnitude at *K*; (2) significantly reddened in that the star had no, or only a very faint, optical counterpart; and (3) located in the region of B216–217 which is inaccessible to optical polarimetry.

The polarization observations were carried out in September of 1991 at the IRTF, using MIRP (cf. Jones & Klebe 1988). In each integration, we sought to achieve an error of less than one part in eight in the percentage polarization, which corresponds to an uncertainty in the polarization position angle of

less than about 4° (Serkowski 1974). Linear polarization was measured for 22 stars, seven in *J* and 15 in *K* (see Table 1). The choice of wavelength depends on two competing trends. Stars polarized by interstellar dust give a larger percentage polarization at the shorter infrared wavelengths (Wilking, Lebofsky, & Rieke 1982), but highly reddened stars are brighter at the longest wavelength. Polarizations measured at *J* have been adjusted to *K* values in the column labeled “*p_K*” in Table 1. The correction factor used (× 1/3) is nearly constant, and it is independent of the wavelength of maximum polarization (Wilking et al. 1982). For three stars, we measured linear polarization at *J*, *H*, and *K*, and the implied wavelength dependence agrees with Wilking et al. (1982).

3. RESULTS

The polarization maps presented in Figure 1 clearly show that the polarization direction and dispersion observed to be associated with B216–217 in the near-infrared is very similar to what could be extrapolated from the optical polarimetry around the cloud periphery.

Figure 2 makes it plain that the distributions of polarization position angles for the optical and infrared data are remarkably similar. The Kolmogorov-Smirnoff two-sample, two-tailed test indicates that the distributions are indistinguishable at a significance level better than 0.01 (Siegel 1956). Myers & Goodman (1991, hereafter MG) have modeled the dispersion

TABLE 1
NEAR-INFRARED POLARIMETRY IN THE B216–217 DARK CLOUD REGION

R.A.(1950) (1)	Decl.(1950) (2)	<i>p_K</i> (3)	<i>σ_{p_K}</i> (4)	<i>θ_E</i> (5)	<i>σ_{θ_E}</i> (6)	Instrument (7)	Band (8)	<i>m_J</i> (mag) (9)	<i>m_K</i> (mag) (10)	<i>J–K</i> (mag) (11)
Polarized Background Stars										
4 ^h 19 ^m 19 ^s .7	26°39'26"	0.76%	0.07%	13°	3°	MIRP	J	11.4	9.8	1.6
4 19 43.6	26 38 54	1.39	0.09	26	7	RC2	K	12.0	9.4	2.6
4 20 3.6	26 42 32	0.38	0.06	52	5	MIRP	J	12.3	11.2	1.1
4 20 11.7	26 36 24	1.04	0.29	28	7	RC2	K	12.1	10.5	1.6
4 20 14.0	26 34 19	0.91	0.13	21	7	RC2	K	12.8	10.2	2.6
4 20 41.6	26 35 53	0.87	0.12	3	4	MIRP	K	12.1	9.3	2.8
4 20 46.0	26 33 13	0.80	0.16	13	6	MIRP	K	13.4	11.0	2.4
4 20 47.6	26 41 21	0.51	0.06	8	3	MIRP	J	8.4	7.0	1.4
4 20 52.4	26 29 44	0.98	0.12	40	3	MIRP	K	12.0	10.1	1.9
4 20 55.3	26 43 11	0.41	0.05	13	4	MIRP	J	9.3	8.2	1.1
4 21 6.6	26 25 10	0.79	0.18	47	6	MIRP	K	12.2	10.6	1.6
4 21 27.8	26 21 53	1.29	0.09	43	2	MIRP	J	12.3	11.1	1.2
4 21 29.3	26 26 45	0.65	0.08	35	4	MIRP	J	11.8	10.6	1.2
4 21 34.8	26 20 00	1.33	0.11	50	7	RC2	K	10.2	9.2	1.0
4 21 46.3	26 22 5	0.99	0.05	43	1	MIRP	J	9.8	9.0	0.8
4 22 11.6	26 22 25	1.01	0.20	33	6	MIRP	K	13.7	11.8	1.9
4 22 32.2	26 12 58	0.65	0.12	39	5	MIRP	K	12.0	11.1	0.9
4 22 34.1	26 22 46	1.47	0.26	25	5	MIRP	K	12.8	11.1	1.7
Embedded Objects ^a										
4 18 57.5	26 50 29	1.54	0.11	69	7	RC2	K	11.2	8.0	3.2
4 21 24.9	26 33 23	0.65	0.12	149	5	MIRP	K	12.3	11.0	1.3
Unpolarized Sources ^b										
4 20 9.8	26 41 26	0.24	0.24	MIRP	K	12.6	11.1	1.5
4 20 16.9	26 39 38	0.35	0.35	MIRP	K	12.0	10.6	1.4

NOTES.—Col. (3), polarization at 2.2 μm; col. (4), error in *σ_{p_K}*; col. (5), position angle of polarization, measured E of N; col. (6), error in *θ_E*, calculated according to, *σ_{θ_E}* = 28°6 [σ_{*p*}/*P*] (Serkowski 1974); col. (7), instrument used to measure polarization; col. (8), band of polarization observations, measurements at *J* have been scaled by × 1/3 to correct to *p_K* (see § 2.2); col. (9), magnitude at 1.3 μm; col. (10), magnitude at 2.2 μm; col. (11), *m_J* – *m_K*.

^a These objects were identified as embedded from their *J*, *H*, *K* colors—they are not included in Fig. 1.

^b These objects have *σ_{p_K}* ≥ *p_K* and are shown as asterisks in Fig. 1.

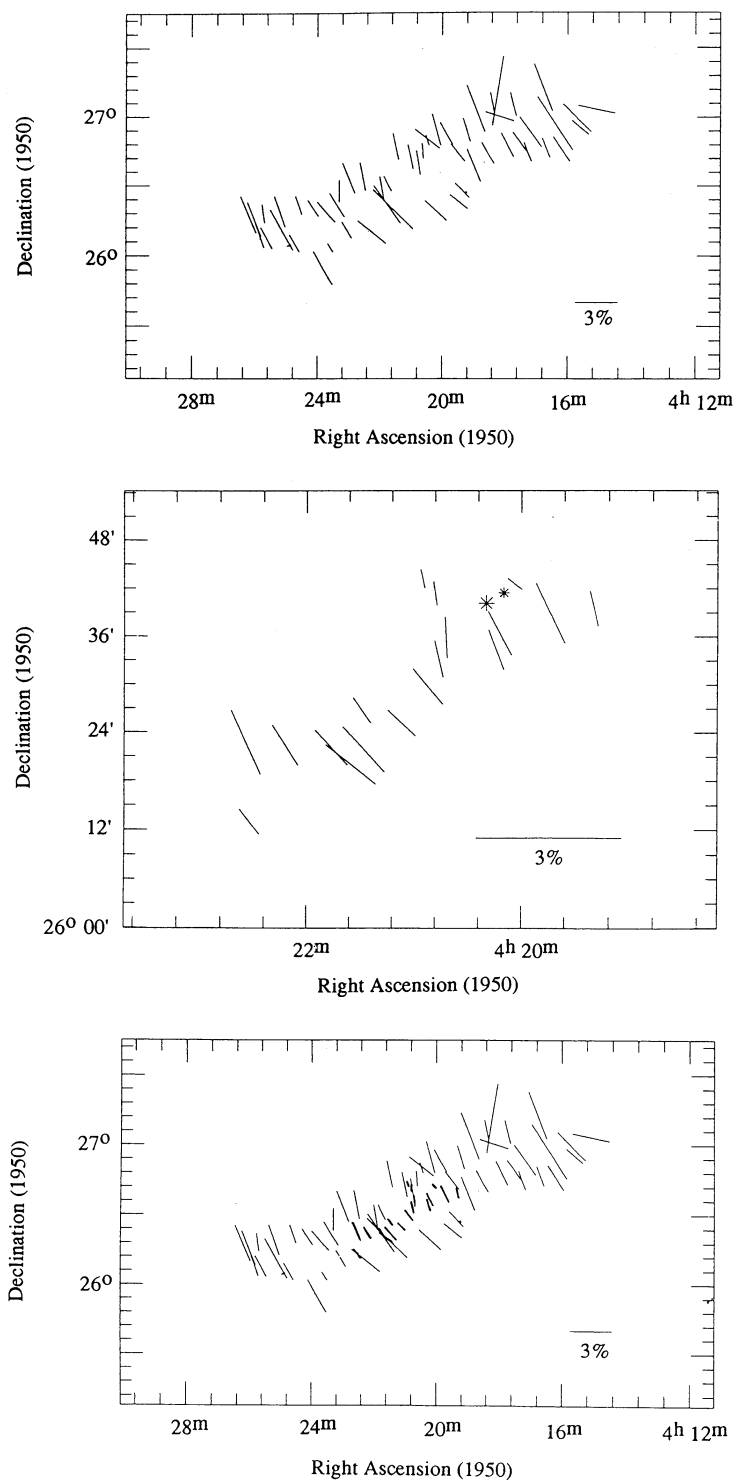


FIG. 1.—*Top*: Optical polarization map of the B216–217 dark cloud, based on Heyer et al. 1987. *Middle*: Infrared polarization map of the B216–217 dark cloud, based on the data in Table 1; the two unpolarized stars are shown as asterisks (*), whose size is proportional to the limit on p_R . *Bottom*: Superposition of optical and infrared polarimetry based on the data shown in the two panels above. Note that the infrared data have been darkened in the bottom panel, and unpolarized sources are not shown. The length of the vectors is proportional to p_R for the infrared data, and p_V for the optical data, with the scale as indicated, in all panels.

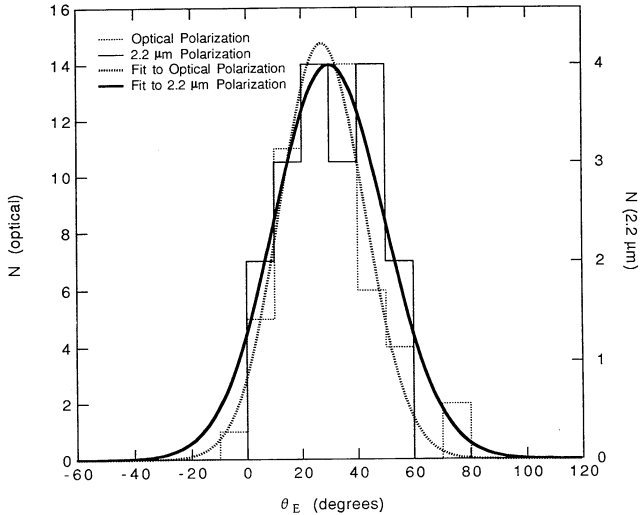


FIG. 2.—Dispersion in polarization position angle in the dark cloud B216–217. Fits of the MG model described in § 2 give $\bar{\theta}_E = 27^\circ \pm 1^\circ$ and $s = 0.27 \pm 0.01$ for the optical data, and $\bar{\theta}_E = 31^\circ \pm 2^\circ$ and $s = 0.31 \pm 0.03$ for the infrared data.

in direction of interstellar polarization, with the assumption that the field can be represented by the vector sum of a uniform (straight) field, B_o , and a nonuniform field, which has a Gaussian-random distribution of amplitudes, characterized by a 1σ dispersion σ_B . In most circumstances (see MG for details), the observed distribution of polarization position angles can be approximated by a Gaussian, with center $\bar{\theta}_E$, and 1σ width s radians, where

$$s = \frac{\sigma_B}{N^{1/2} B_o} \quad (1)$$

and N is the number of field correlation lengths along the line of sight. The smooth curves in Figure 2 represent fits of the MG model to both the optical and infrared data. The optical data give $\bar{\theta}_E = 27^\circ \pm 1^\circ$ and $s = 0.27 \pm 0.01$, while the infrared data give $\bar{\theta}_E = 31^\circ \pm 2^\circ$ and $s = 0.31 \pm 0.03$. Thus, the distributions are also indistinguishable within the framework of the MG model.

4. DISCUSSION

4.1. A Continuous, Uniform Field?

The most obvious conclusion to draw upon inspection of Figure 1 is that the magnetic field in the vicinity of B216–217 is unaffected by the presence of the dark cloud. In this interpretation, the field lines continue “straight-through” the cloud, with no change in their density or direction, implying that whatever process(es) formed the cloud (i.e., gravitational collapse, instability, agglomeration, etc.) did not also affect the field structure. This interpretation implies that the energy density in the uniform field in the cloud is the same as in its environment, and that the uniform component of the magnetic field does not help support the cloud against self-gravity. It is difficult to reconcile this conclusion with Zeeman measurements of uniform field strength, which often imply a magnetic energy density comparable to the kinetic and gravitational energy densities in interstellar clouds (Myers & Goodman 1988; Goodman et al. 1989).

4.2. Undetected Field Variations

It is possible that the magnetic field structure is affected by the presence of the B216–217 dark cloud, but that infrared polarimetry cannot reveal the effects. If either the polarizing effectiveness of the grains is low, and/or the field direction decorrelates several times within the cloud, polarimetry would be insensitive to the details of the true field structure.

Even though the bulk of the extinction along lines of sight through a dark cloud is from the densest regions, it is not necessarily the case that the polarization we observe originates in those regions. So, we must analyze the amount of polarization produced, as a function of extinction. To evaluate polarization efficiency, p_K/A_V , we evaluate the dependence of K -band polarization, p_K , on visual extinction, A_V . In B216–217, A_V is estimated using the relationship $A_V = 5.6[(J-K) - 1]$, where it is assumed that background stars are K or M giants with an intrinsic $(J-K)$ of about 1 mag (see Jones 1989, and references therein). This method is not as accurate as calculating reddening for stars of known spectral type, and we estimate that errors of ± 1 mag are not uncommon.

Figure 3 shows the relationship between p_K and A_V in the B216–217 region, based on the data in Table 1. Also shown in the figure are the results of similar K -band polarization observations by Wilking et al. (1979) in the ρ Ophiuchus cloud and by Tamura et al. (1987) in Heiles Cloud 2. A weighted least-squares fit of a power law to the all of the data in Figure 3 gives $p_K = 10^{-0.3 \pm 0.3} A_V^{0.5 \pm 0.3}$. (An unweighted fit gives the same coefficient and exponent, with errors 5 times smaller.) As is evident in Figure 3, the B216–217 data alone are not well-fit by a simple power law; nonetheless, an unweighted least-squares fit to only these points has power-law slope ~ 0.3 . We caution that changes in the inclination of the uniform field to the line of sight can cause variations in p_K/A_V from region to region. However, such effects are not likely to be responsible for the shallow slopes deduced from Figure 3, especially given

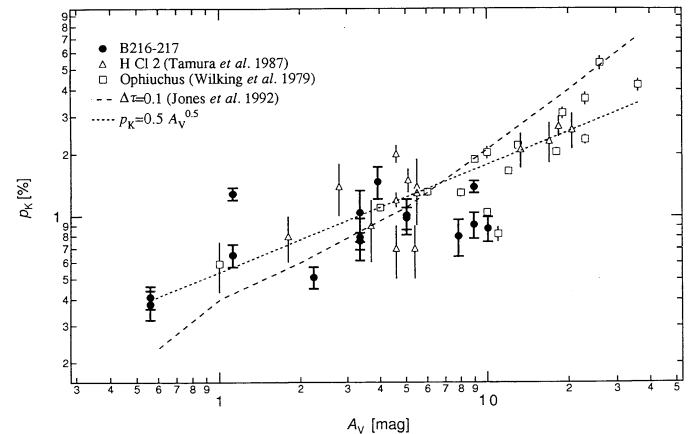


FIG. 3.—Relationship between p_K and A_V in the B216–217 region, ρ Ophiuchus (Wilking et al. 1979), and Heiles Cloud 2 (Tamura et al. 1987). For B216–217, A_V is calculated from the $J-K$ data in Table 1, using the expression $A_V = 5.6[(J-K) - 1]$, and we estimate that errors of ± 1 mag are appropriate (see § 4.2). Errors in A_V in H Cl 2 are similar to those in B216–217, and significantly smaller in ρ -Oph. Also shown are a least-squares fit to all the data in the figure ($p_K = 0.5 A_V^{0.5}$), and the Jones et al. (1992) model where it is assumed that there is equal energy in uniform and nonuniform field, and that the decorrelation optical depth for the field, $\Delta\tau$, is 0.1 mag at K , which corresponds to approximately 1 mag A_V .

that two clouds (H Cl 2 and B216–217) out of the three included are quite near each other, in the Taurus dark cloud complex.

Jones, Klebe, & Dickey (1992; see also Jones 1989) have compiled additional *K*-band polarization and extinction measurements, which also include non-dark cloud lines of sight, in an attempt to model the nature of the Galactic Magnetic Field. A shallower-than-linear dependence of p_K on A_V (for $A_V < 100$; see Jones 1989) implies either a decrease in polarization efficiency as a function of column density, and/or change(s) in field direction along the line of sight. Jones et al. consider primarily the latter possibility, but it is probably necessary to consider both polarization efficiency and field geometry in analyzing dark clouds.

In the models of Jones et al. and MG, the field is comprised of uniform and nonuniform parts. The correlation of p_K and A_V found by Jones (1989) can be fit with a power-law where $p_K = 10^{-0.44} A_V^{0.75}$. Although this power-law characterizes the overall trend in the data, Jones and Jones et al. suggest that the correlation is best explained by a model in which the nonuniform field decorrelates each time an optical depth length $\Delta\tau$ is traversed along the line of sight, and where there is approximately equal energy in the uniform and nonuniform field. The results of such a model are illustrated in Figure 3. Note that unity alignment efficiency and a perfectly uniform field would give a slope of 1 in Figure 3, and zero alignment efficiency would give a slope of 0.

The power law we fit to the exclusively dark cloud data in Figure 3 is significantly flatter than the data modeled in Jones and Jones et al., giving an exponent of ~ 0.5 , and at most 0.3 in the data for B216–217 alone. In the model of Jones et al., which can explain the relationship between polarization and extinction primarily with field geometry arguments, and is not especially sensitive to variations in polarization efficiency, an exponent of 0.5 corresponds to a purely random field, with no uniform component. We know this situation is ruled out, given the large-scale coherent structure we see in the polarization maps. In addition, the Jones et al. model predicts a narrowing of the dispersion in polarization position angle with increasing optical depth, which is also inconsistent with our results (see Fig. 2). Thus, we conclude that field geometry alone cannot explain the shallow power-law correlation of p_K and A_V in B216–217 and other dark clouds, and that a decrease in polarizing efficiency with increasing extinction is likely.

If grains are poorly aligned, and/or they are poor polarizers in dense regions, then the overall polarization efficiency there will be reduced. The efficiency of grain alignment in a dense cloud might be low due to disorienting collisions, low gas/dust temperature ratio, gas streaming, and/or insufficient grain magnetization (see Hildebrand 1988 and Gonatas et al. 1990). It is also possible that the distribution of grain size, shape, and/or composition in dense regions causes a lower polarizing efficiency, even if grains are aligned. If polarization efficiency is diminished in dense regions, then much of the polarization observed in the near-infrared arises in “ambient” (i.e., lower-density) material, and it is possible that infrared polarization maps may be somewhat misleading, in that the field traced is not necessarily representative of that existing in the densest gas.

On the other hand, far-infrared polarization observations in the Orion molecular cloud (Novak et al. 1989; Gonatas et al.

1990), which depend solely on *emission from dust in dense regions*, give field directions in good agreement with those based on optical observations of background stars. To resolve this paradox, we will need to wait for far-infrared polarimetric measurements of dust emission from dark clouds like B216–217, which will allow for more direct comparisons of optical, near-infrared, and far-infrared data.

The similarity of the optical and near-infrared polarization maps of B216–217 appears unlikely to arise solely from the statistical and geometrical effects discussed by Jones, Jones et al., and MG. The Jones et al. model predicts a narrowing of the distribution of observed polarization position angle as density increases, which is not seen in dark clouds thus far, and a steeper slope (> 0.5) for p_K versus A_V than what is observed (< 0.3). In the MG model (see eq. [1]), the fields inside and outside the cloud could have the same uniform component, B_o , but different nonuniform components, provided the dispersion σ_B of the nonuniform field and the number, N , of field correlation lengths along the line of sight are in the relation $(\sigma_B/\sqrt{N})_{\text{inside}} = (\sigma_B/\sqrt{N})_{\text{outside}}$. A physically motivated explanation of such a relation is not immediately obvious.

5. CONCLUSIONS

There are now at least three examples (B216–217, H Cl 2, and ρ Oph) of dark clouds where near-infrared polarimetry reveals a pattern of polarization vectors very similar in direction and dispersion to those measured optically in the lower-extinction gas around the periphery of the clouds. There are two possible explanations for these results. First, it is possible that the field lines pass “straight-through” the dark clouds, with no change in their spacing or direction. Yet magnetic fields are often energetically significant in dark clouds (e.g., Myers & Goodman 1988; Goodman et al. 1989), so it seems somewhat unlikely that the ambient field structure would be completely unchanged due to the presence of a dark cloud. Alternatively, either low polarization efficiency or field nonuniformity, or both, lead to polarization maps which do not reveal the change in field structure due to a dark cloud.

To discriminate among these alternatives, more information is required. Foremost, we need to map more dark clouds with near-infrared polarimetry. Spectropolarimetry will allow better evaluation of the polarizing power of dust in different regimes. More refined models of the p_K – A_V relationship should include cloud-to-cloud variations in the relationship observed, as well as detailed consideration of the effects of variations in grain composition, and in field orientation with respect to the line of sight (see Jones et al.). In addition, far-infrared polarization observations of dark clouds are needed, preferably extended maps which can likely only be made outside the Earth’s atmosphere. With this additional information, it will be possible to assess the generality of the current results which indicate that polarized emission from dust in very dense regions implies the same field direction present in the ambient (lower density) clouds.

We thank Bruce Draine, Bruce Elmegreen, Carl Heiles, Chris McKee, Boqi Wang, and Ellen Zweibel for their insights concerning these results. In addition, we are grateful to Geoff Lawrence for his assistance in resurrecting MIRC at the IRTF, and Ron Probst for his useful advice at KPNO. T. J. acknowledges support for MIRC from NSF grant AST 8912803.

REFERENCES

- Davis, L., Jr., & Greenstein, J. L. 1951, *ApJ*, 114, 206
Fowler, A. M., et al. 1987, *Opt. Engineering*, 26, 232
Goodman, A. A., Bastien, P., Myers, P. C., & Ménard, F. 1990, *ApJ*, 359, 363
Goodman, A. A., Crutcher, R. M., Heiles, C., Myers, P. C., & Troland, T. H. 1989, *ApJ*, 338, L61
Gonatas, D. P., et al. 1990, *ApJ*, 357, 132
Heyer, M. H. 1988, *ApJ*, 324, 311
Heyer, M. H., et al. 1987, *ApJ*, 321, 855
Hildebrand, R. H. 1988, *QJRAS*, 29, 327
Jones, T. J. 1989, *ApJ*, 346, 728
Jones, T. J., & Klebe, D. I. 1988, *PASP*, 100, 1158
Jones, T. J., Klebe, D., & Dickey, J. M. 1992, *ApJ*, submitted
Lada, E. A., DePoy, D. L., Evans, II, N. J., & Gatley, I. 1991, *ApJ*, 371, 171
Moneti, A., Pipher, J. L., Helfer, H. L., McMillan, R. S., & Perry, M. L. 1984, *ApJ*, 282, 508
Myers, P. C., & Goodman, A. A. 1988, *ApJ*, 326, L27
———. 1991, *ApJ*, 373, 509 (MG)
Novak, G., Gonatas, D. P., Hildebrand, R. H., & Platt, S. R. 1989, *ApJ*, 345, 802
Purcell, E. M. 1979, *ApJ*, 231, 404
Serkowski, K. 1974, *Methods of Experimental Physics*, (NY: Academic Press)
Siegel, S. 1956, *Nonparametric Statistics for the Behavioral Sciences* (NY: McGraw-Hill)
Tamura, M., Nagata, T., Sato, S., & Tanaka, M. 1987, *MNRAS*, 224, 413
Wilking, B. A., Lebofsky, M. J., & Rieke, G. H. 1982, *AJ*, 87, 695
Wilking, B. A., Lebofsky, M. J., Rieke, G. H., & Kemp, J. C. 1979, *AJ*, 84, 199